Vol 16 No 12, December 2007
1009-1963/2007/16(12)/3790-08

Chinese Physics

© 2007 Chin. Phys. Soc.
and IOP Publishing Ltd

Tribological properties of diamond-like carbon films deposited by pulsed laser arc deposition*

Zhang Zhen-Yu(张振宇)[a)b)†], Lu Xin-Chun(路新春)[a)], and Luo Jian-Bin(雒建斌)[a)]

[a)] *State Key Laboratory of Tribology, Tsinghua University, Beijing* 100084, *China*
[b)] *Key Laboratory for Precision and Non-Traditional Machining Technology of the Ministry of Education, Dalian University of Technology, Dalian* 116024, *China*

(Received 21 January 2007; revised manuscript received 23 May 2007)

A novel method, pulsed laser arc deposition combining the advantages of pulsed laser deposition and cathode vacuum arc techniques, was used to deposit the diamond-like carbon (DLC) nanofilms with different thicknesses. Spectroscopic ellipsometer, Auger electron spectroscopy, x-ray photoelectron spectroscopy, Raman spectroscopy, atomic force microscopy, scanning electron microscopy and multi-functional friction and wear tester were employed to investigate the physical and tribological properties of the deposited films. The results show that the deposited films are amorphous and the sp^2, sp^3 and C–O bonds at the top surface of the films are identified. The Raman peak intensity and surface roughness increase with increasing film thickness. Friction coefficients are about 0.1, 0.15, 0.18, when the film thicknesses are in the range of 17–21 nm, 30–57 nm, 67–123 nm, respectively. This is attributed to the united effects of substrate and surface roughness. The wear mechanism of DLC films is mainly abrasive wear when film thickness is in the range of 17–41 nm, while it transforms to abrasive and adhesive wear, when the film thickness lies between 72 and 123 nm.

Keywords: pulsed laser arc deposition, diamond-like carbon, tribological property, physical property
PACC: 6855, 6115J, 6170T

1. Introduction

Diamond-like carbon (DLC) or amorphous carbon films are well-known for their attractive properties, such as low friction coefficient, high wear resistance, chemical inertness and biocompatibility.[1,2] At present, the deposition methods of DLC are mainly as follows: ion deposition, ion-assisted deposition, sputtering, cathodic vacuum arc (CVA), plasma deposition and pulsed laser deposition (PLD).[3] Pulsed laser arc deposition (PLAD) is a novel method hybridizing the techniques of PLD and CVA,[4,5] and overcomes their shortcomings. For example, PLD has a low deposition rate and high positioning precision, while CVA has a high deposition rate and low positioning precision. PLAD has the advantages of those in PLD and CVA, such as high deposition rate and positioning precision, and is successfully used to deposit Al-CuFe quasicrystalline[4] with high quality. Whereas, the change rule of tribological properties with film thickness of DLC nanofilms prepared by using this method has not been reported, which is the deposition basis for DLC nanofilms doped with a third element, such as rare earth metal with excellent tribological properties,[6−8] by using this novel method. In this paper, the tribological and physical properties of DLC films versus film thickness are presented.

2. Experiment details

2.1. Preparation of DLC films

DLC nanofilms were deposited using a novel pulsed laser arc deposition technique developed in our laboratory, LAD-300, as shown in Fig.1.[4,5] A Si (100) plane was selected as substrate supersonically cleaned in acetone for 10 min prior to mounting on the substrate holder imbedded with a heater for controlling the substrate temperature in the range of 300–700 K via an adjustable resistor. A graphite target (purity

*Project supported by the National Key Basic Research Program of China (Grant No 2003CB716201), the Major Research Plan of the National Natural Science Foundation of China (Grant No 50390060), the National Natural Science Foundation of China (Grant No 50575121), the National Science Foundation for Post-doctoral Scientists of China (Grant No 20060390064), the Electro-Mechanic Technology Foundation of NSK Ltd. of Japan, the Scientific Startup Research Foundation for the New Staff of Dalian University of Technology, and the Open Foundation of Key Laboratory for Precision and Non-Traditional Machining Technology of the Ministry of Education, Dalian University of Technology (Grant No JMTZ200703).
†E-mail: zzy@dlut.edu.cn

99.99%) as target cathode was installed on the target holder, connected with a ring anode. Its internal diameter is 10 mm, outer diameter 12 mm and parallel to the target surface through pulsed current circuit. Then the chamber was closed and evacuated to a base pressure, lower than 9.8×10^{-4} Pa. Prior to deposition, argon ions generated under the argon gas pressure at 3.5 Pa, was used to sputter the substrate for 10 min to eliminate the oxide layer. The sputtering was operated at the substrate bias voltage of 400 V and anode voltage of 800 V. The heater resistor was adjusted to 60 V for 20 min to heat the substrate to 473 K, then interruptedly heating for 30 s at intervals of 5 min during the process of deposition. The deposition was carried out at the substrate bias voltage of 200 V, anode voltage of 1000 V with a Nd-YAG pulsed laser beam with frequency (1, 3, 5 and 10 Hz, respectively) at 1 Hz. Under the action of pulsed laser and the electric field between the ring anode and target cathode, laser-induced plasma was emitted to initiate the vacuum arc that further stimulated the emission of more plasma from the vicinity of the target. The arc pulse duration was controlled by a specially designed pulse arc source so as to obtain controllable ablation of the target. With the deposition going on, the target could be moved in the two-dimensional plane to reduce the consumption of the target and make the deposited film grow evenly. This function could also be used to make a precise multi-target deposition, in which the motion of the target was controlled by a step motor through a programmed procedure. The film thickness could be controlled precisely within the time from 8 to 58 min.

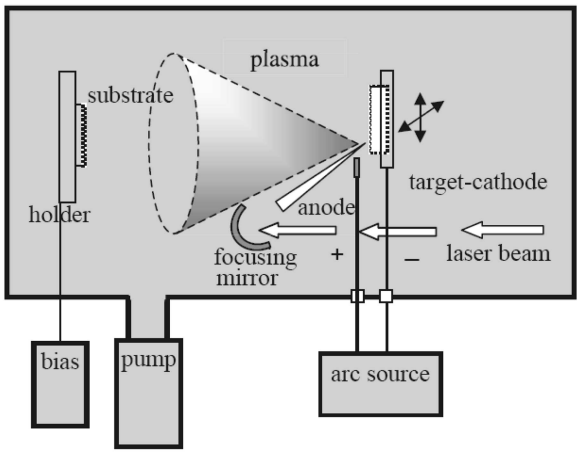


Fig.1. Schematic diagram of home-made LAD-300 system.

2.2. Characterization methods

The film thickness was measured by a spectroscopic ellipsometer (GES-5, Sopra, France) with wavelength 300–900 nm and refractive index 1.7–2.6.[9] Raman spectroscopy was obtained using a microscopic confocal Raman spectrometer (Renishaw 1000, UK) with 514 nm Ar^+ laser operated at a power of 5 mW, a 50× objective, exposure time of 30 s and the accumulated times of 6. Chemical bonding in the film was determined by x-ray photoelectron spectroscopy (XPS) (Quantera, ULVAC-PHI, Japan). Chemical composition and element distribution along depth direction were investigated by Auger electron spectroscopy (PHI-700, ULVAC-PHI, Japan). Surface morphology and roughness were characterized by atomic force microscopy (AFM, SPA-300HV, Seiko, Japan) operated under tapping mode, and the report of surface roughness Ra is the average of three readings. Wear tracks were observed by an environmental scanning electron microscopy (SEM, FEI Quanta 200 FEG, Netherlands) equipped with energy disperse x-ray spectroscopy (EDS). Friction coefficient was obtained by a ball-on-block multi-functional friction and wear tester (UMT, CETR, USA) under unlubricated condition, at room temperature, in ambient air. The applied load was 100 mN, sliding distance 5 mm, sliding speed 0.167 mm/s and duration 30 s. A chromic steel ball with a diameter of 1.6 mm was selected as the counterpart. For each film, a new ball was supersonically cleaned in the acetone solution for 10 min, then mounted on the ball holder to start a new experiment, and ten tests were conducted under the same parameters and the interval distance is 2 mm. For each test, the chromic steel ball was supersonically cleaned in the acetone solution for 1 min to eliminate the wear debris and adjusted to a new location.

3. Results and discussion

3.1. XPS spectra

Figure 2 shows the XPS spectra of C 1s and O 1s photoelectron peaks for DLC nanofilm with a thickness of 43 nm. To know the chemical bonding states of DLC nanofilm, the individual C 1s line is deconvoluted into three Gaussian line shapes. The deconvoluted C 1s spectrum of the DLC nanofilm exhibits three peaks at binding energies of 283.5, 285.3 and

287.8 eV (Fig.3(a)). Merel *et al*[10] and Fei *et al*[11] have indicated that the first peak at 283.5 eV corresponds to sp^2 carbon atoms, while the second peak at 285.3 eV corresponds to sp^3 carbon atoms. The third peak at 287.8 eV is attributed to some C-O contamination formed on the DLC nanofilm surface. So the sp^2 and sp^3 bonds showing the DLC nature characteristics are identified.

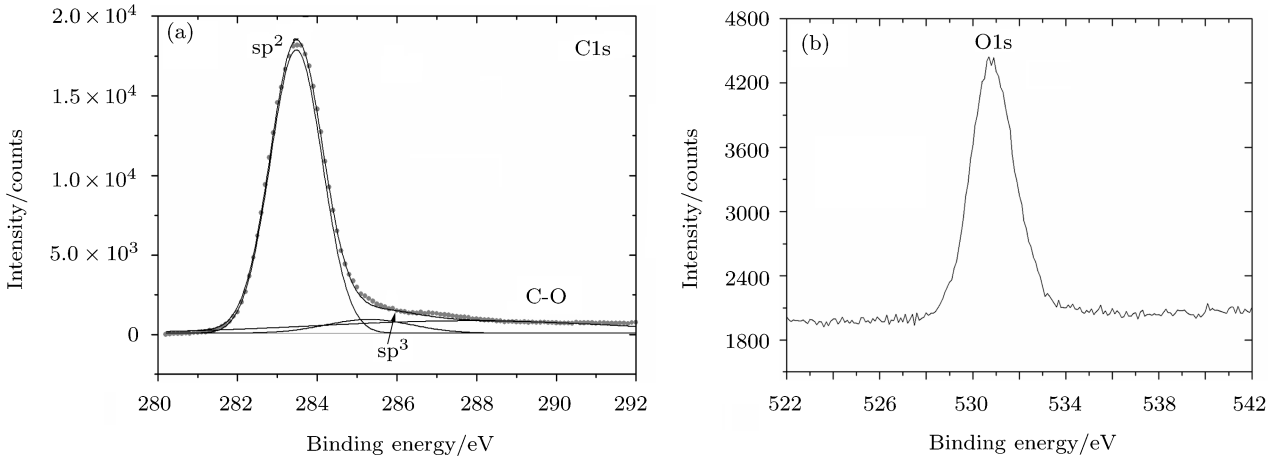


Fig.2. XPS spectra of C 1s and O 1s photoelectron peaks for DLC nanofilm with a thickness of 43 nm.

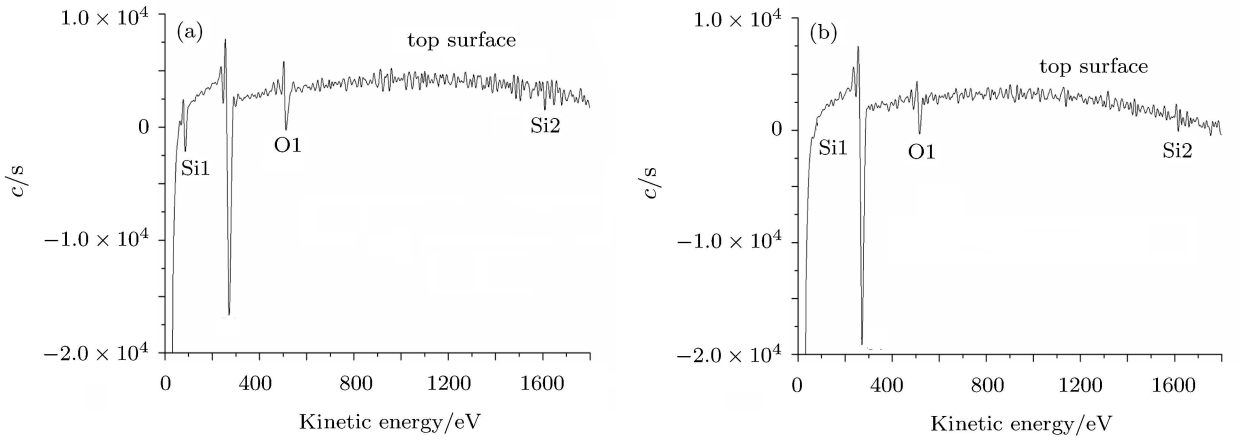


Fig.3. AES spectra for top surface of deposited films of thickness (a) 28 nm and (b) 44 nm.

3.2. AES spectra

Figure 3 shows the AES spectra of top surface of the deposited films. Si, O and C peaks are observed in AES spectra of two films. The appearance of oxygen element is consistent with the results of XPS. Inclusion of Si is suggested that diffusion from the substrate have occurred. Also considering the existence of Si and O elements, these peaks may originate from the native oxide layer of Si substrate. Furthermore, the AES spectra are the clear evidence of C KLL peak at 268 eV.[12] Figures 4(a) and 4(b) show the Auger depth profiles of DLC nanofilms with thicknesses of 28 and 44 nm, respectively. It is apparent from both pictures that the element distributions along depth direction are uniform, and carbon atoms have penetrated into the substrate and a mixed zone at the interface has been formed. Furthermore, the existence of oxygen element with small percentage at the interface is observed, which is attributed to the formation of a thin film of silicon oxide before deposition and it cannot be eliminated completely by Ar^+ bombardment.

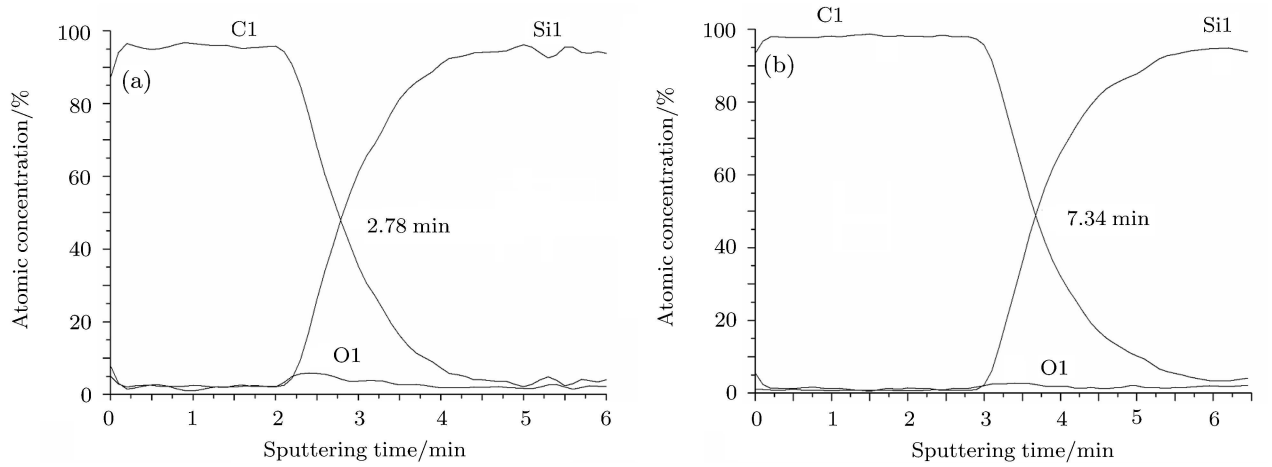


Fig.4. Auger depth profiles of DLC nanofilm with thickness of (a) 28 nm and (b) 44 nm.

3.3. Raman measurements

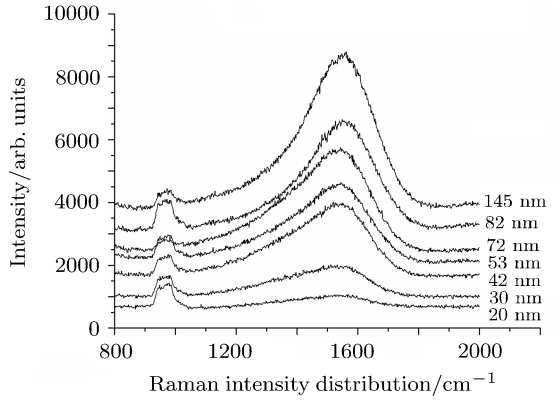


Fig.5. Visible Raman spectra for DLC films with varied thicknesses.

Figure 5 shows the Raman spectra of DLC films with thickness ranging from 17 to 145 nm. The spectra exhibit an asymmetric broad Raman intensity distribution in the range of 1100–1900 cm^{-1} centred at about 1550 cm^{-1}, indicating the obviously amorphous DLC characteristic.[13,14] It is obvious that the peak intensity increases with increasing film thickness. The spectra also show a clear peak at about 965 cm^{-1} regardless of the thickness of the film. This peak corresponds to the second-order phonon scattering from the silicon substrate.[15] The appearance of this peak is a measure of the transparency of the film near the wavelength of 514 nm. The transparency of these films is due to the high fraction of sp3 bonds.[15] The wide peak (1100–1900 cm^{-1}) can be fitted with two Gaussian peaks: a 'G' band at 1560 cm^{-1}, and a 'D' feature at approximately 1360 cm^{-1}. Figure 6 illustrates the fitted peak shift and intensity versus film thickness. The fitted peak intensity increases as the film thickness increases. While, the intensity increases sharply in the range of 17–43 nm, thereafter the intensity increases slowly. Furthermore, the fitted peak shift increases rapidly as the film thickness increases in the range of 21–35 nm, then fluctuates at about 1545 cm^{-1}, when the film thickness varies between 35 and 51 nm, and finally fluctuates at about 1554 cm^{-1}, with the film thickness increasing from 51 to 145 nm. Figure 7 shows the fitted curve with two Gaussian components for the deposited DLC films with varied thickness. As the laser energy of 514 nm is sufficient to excite the σ states of both sp^2 and sp^3 sites.[16,17] It allows the Raman spectrum to show a more equally weighted view of vibrational density of states for sp^2 and sp^3 sites. Therefore, the sp^3 content can be obtained through the quantitative analysis of Raman spectra.[18] Figure 8 shows the intensity ratio (I_D/I_G) as a function of film thickness. I_D/I_G decreases with the increase of film thickness, which implies the increase of sp^3 fraction. This may be attributed to the increase of film stability with the increase of film thickness. As the film thickness increases, the deposition time increases, and the film has more time to grow, which may result in the increase of sp^3 fraction.

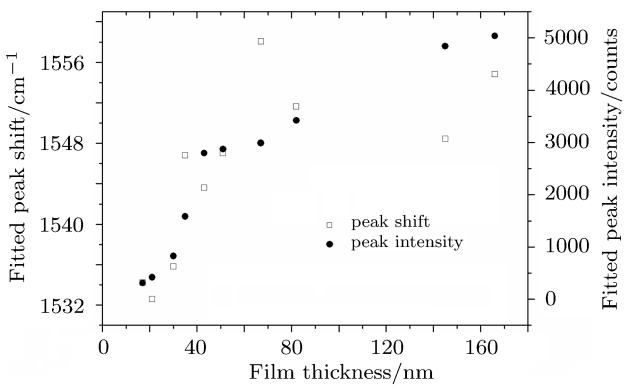


Fig.6. Fitted peak shift and intensity versus film thickness.

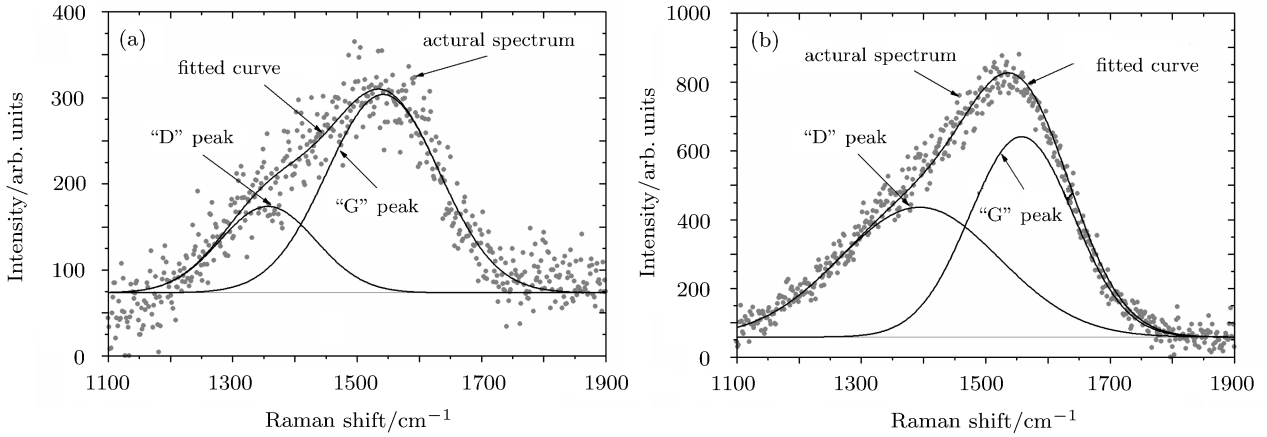


Fig.7. Decomposition of the fitted curve into two Gaussian lines: 'G' and 'D' lines for DLC nanofilms with varied thickness (a) 17 nm and (b) 30 nm.

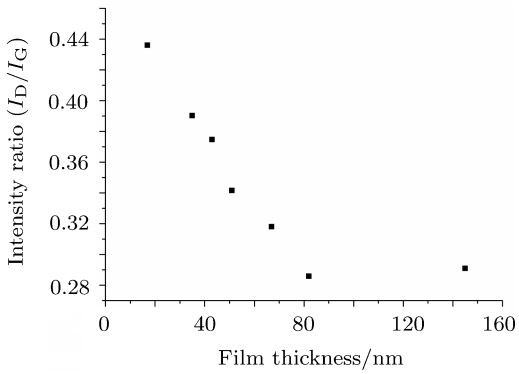


Fig.8. Relative intensity ratio I_D/I_G and sp^3 fraction versus film thickness.

3.4. AFM characterization

Figure 9 shows the AFM morphologies of the top surface of DLC films with different thicknesses. It can be seen that the surface of the film with a thickness of 21 nm is very smooth despite of some bigger grains. While, with increasing thickness, the surface grows coarse and granular and the grains grow bigger gradually. Figure 10 illustrates the variation of surface roughness with the film thickness. It is obvious that the surface roughness increases linearly as the film thickness increases. From Figs.9 and 10, it can be concluded that the growth of films starts from some small particles, then the particles grow gradually with the increase of film thickness, finally some particles glomerate and form a bigger particle. When the film is thinner, the particles are very small and the film is grown of a good quality, so the film surface is very smooth and looks very flat. For example, the 21 nm film has a surface roughness of 1.252±0.038 nm (Fig.10), which is better than the DLC film deposited by magnetron sputtering (1.64 nm).[19] However, the surface will grow coarse as the particles grow bigger.

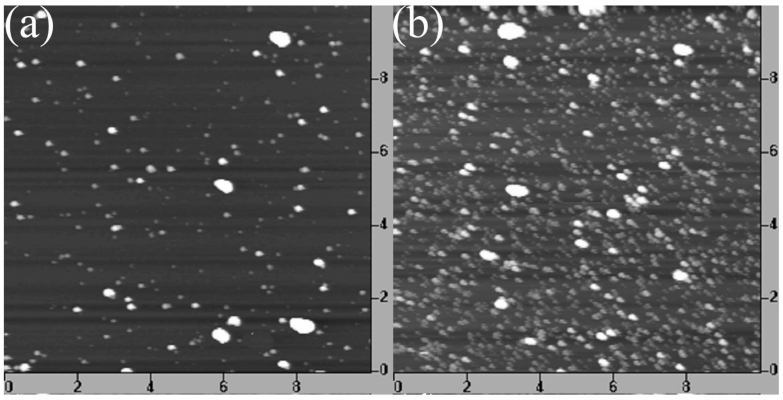


Fig.9. AFM morphologies of top surface of DLC nanofilms with different thicknesses (a) 21 nm and (b) 41 nm.

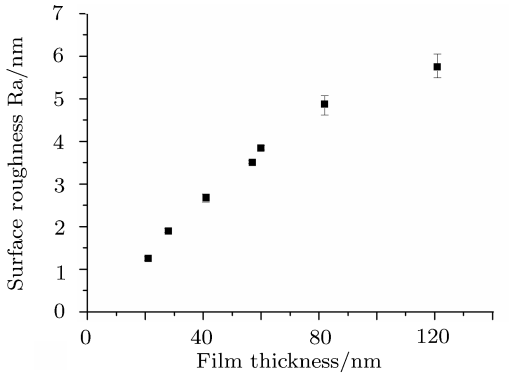


Fig.10. Top surface roughness of DLC nanofilms as a function of film thickness.

3.5. Tribological properties

Figure 11 shows the typical friction coefficient of a DLC film with a thickness of 17 nm. It is obvious that the friction curves have better repeatability. As for the sharp change of friction coefficient in each curve, it corresponds to the end of one sliding direction and returning to the reverse sliding direction. Figure 12 shows the friction coefficient as a function of film thickness. It is found that the friction coefficient stabilizes at about 0.11±0.01, which is lower than that of DLC deposited by filtered cathode vacuum arc (friction coefficients are 0.23 ± 0.03 and 0.16 ± 0.02, when the film thicknesses are 17 and 30 nm, respectively),[13] when the film thickness is between 17 and 21 nm. The friction coefficients are about 0.15 and 0.18, when the film thicknesses lie in the range of 30–57 nm and 67–123 nm, respectively.

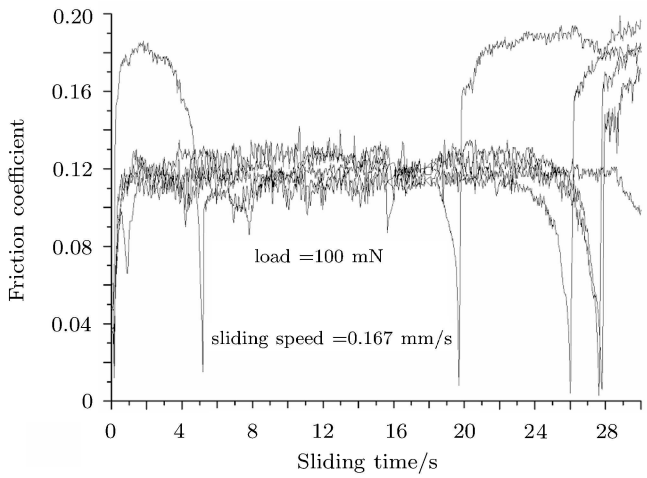


Fig.11. Friction coefficient versus sliding time of 17 nm DLC nanofilm.

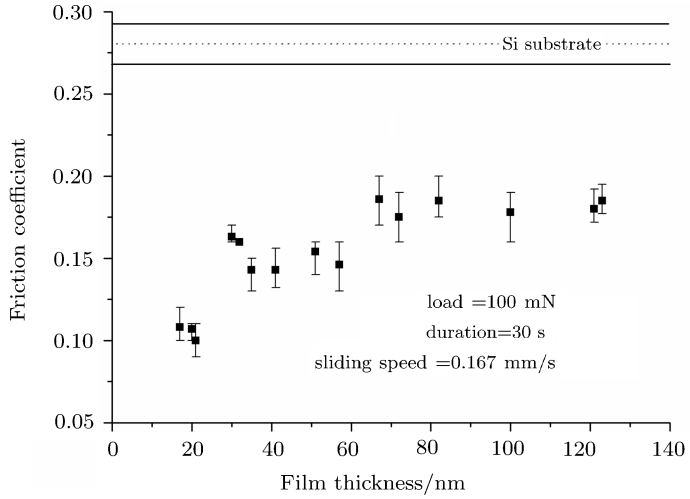


Fig.12. Friction coefficient of DLC nanofilms as a function of film thickness.

From the friction coefficient curve, it is seen that the friction coefficient stabilizes firstly, then increases and stabilizes at some value again, and repeats as the film thickness increases. This is attributed to the interaction between the surface roughness and the substrate effects. As the surface roughness increases, it results in the increase of friction coefficient. When the surface roughness and the film thickness increase the effect of substrate on the film is weakened, and the friction coefficient will decrease. So under the combined effects of substrate and surface roughness, the friction coefficient exhibits the phenomenon as presented above. Figure 13 shows SEM topographies of the worn surface of DLC films with different thicknesses. It is obvious that the wear mechanism of DLC films with thicknesses of 17, 32 and 41 nm is mainly abrasive wear, while that of DLC films with thicknesses of 72, 123 nm is mainly the combination of abrasive wear and adhesive wear. This can be attributed to the disintegration of bigger particles, thus forming the debris which lies in the wear track.

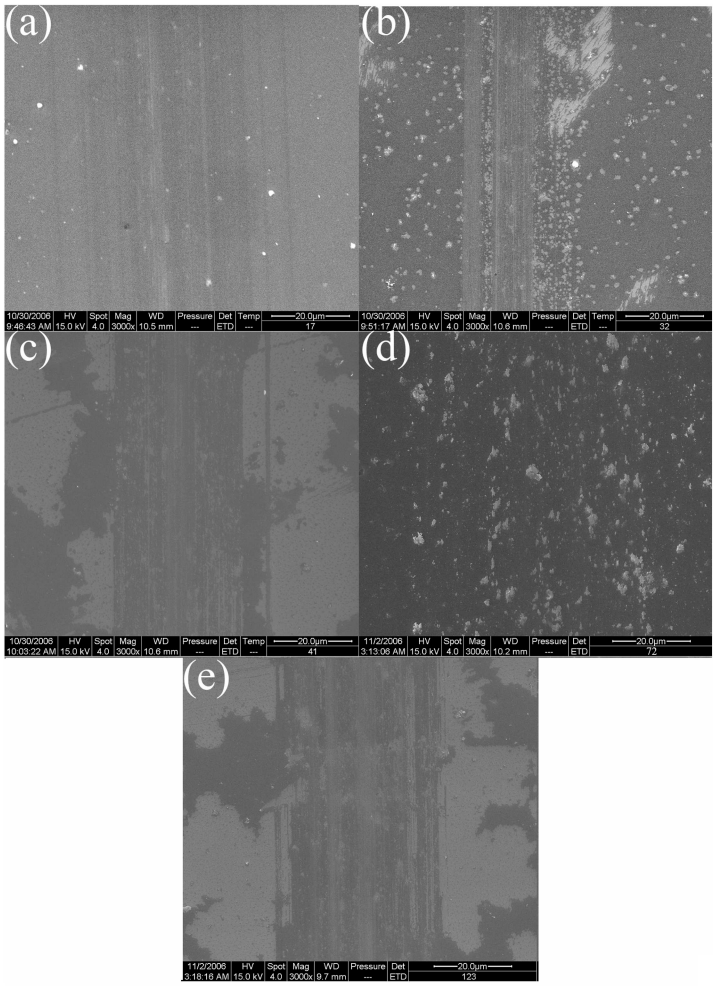


Fig.13. SEM topographies of the worn surface of DLC films with different thicknesses (a) 17 nm, (b) 32 nm, (c) 41 nm, (d) 72 nm and (e) 123 nm.

4. Conclusions

The DLC films have been deposited on silicon substrate using a novel method PLAD. Through the experimental characterizations and measurements, the results obtained are as follows:

1. The surface roughness and Raman peak intensity increase with increasing film thickness.

2. We observed that the film grows from a small particle, and the particle grows as the film thickness increases.

3. The friction coefficient starts and stabilizes at a very low level, then increases and stabilizes with the increase of film thickness, and this process repeats as the film thickness increases. This is attributed to the combined effects of substrate and surface roughness.

4. As the film thickness increases, the wear mechanism may change from abrasive wear to the combination of abrasive and adhesive.

References

[1] Chen L Y and Hong F C N 2003 *Appl. Phys. Lett.* **82** 3526

[2] Wang F L, Jiang J C and Meletis E I 2003 *Appl. Phys. Lett.* **83** 2426

[3] Robertson J 2002 *Mater. Sci. Eng. R Rep.* **37** 129

[4] Sedao, Shao T M, Mou H Q and Hua M 2005 *Thin Solid Films* **483** 1

[5] Zhang Z Y, Lu X C, Luo J B, Shao T M, Qing T and Zhang C H 2006 *Chin. Phys.* **15** 2697

[6] Zhang Z Y, Lu X C and Luo J B 2007 *Appl. Surf. Sci.* **253** 4377

[7] Zhang Z Y, Lu X C, Han B L and Luo J B 2007 *Mater. Sci. Eng.* A **444** 92

[8] Zhang Z Y, Lu X C, Han B L and Luo J B 2007 *Mater. Sci. Eng.* A **454** 194

[9] Dowling D P, Donnelly K, Monclus M and McGuinness M 1998 *Diamond Rel. Mater.* **7** 432

[10] Merel P, Tabbal M, Chaker M, Moisa S and Margot J 1998 *Appl. Surf. Sci.* **136** 105

[11] Fei Z, Koshi A and Koji K 2006 *Thin Solid Films* **514** 231

[12] Sreejith K, Nuwad J and Pillai C G S 2005 *Appl. Surf. Sci.* **252** 296

[13] Zhang Z Y, Lu X C, Luo J B, Liu Y and Zhang C H 2007 *Diamond Rel. Mater.* **16** 1905

[14] Zhang Z Y, Lu X C, Luo J B, Liu Y and Zhang C H 2007 *Surf. Coat. Technol.* doi:10.1016/j.surfcoat.2007.07.018

[15] Friedman T A, McCarty K F, Barbour J C, Siegal M P and Dibble D C 1996 *Appl. Phys. Lett.* **68** 1643

[16] Merkulov V I, Lannin J S, Munro C H, Asher S A, Veerasamy V S and Milne W I 1997 *Phys. Rev. Lett.* **78** 4869

[17] Gilkes K W R, Sands H S, Batchelder D Robertson N J and Milne W I 1997 *Appl. Phys. Lett.* **70** 1980

[18] Tay B K, Shi X, Tan H S, Yang H S and Sun Z 1998 *Surf. Coat. Technol.* **105** 155

[19] Libardi J, Grigorov K, Massi M, Otani C, Ravagnani S P, Maciel H S, Guerino M and Ocampo J M J 2004 *Thin Solid Films* **459** 282